Journal of Sound and Vibration (2001) 243(2), 269–282
doi:10.1006/jsvi.2000.3410, available online at http://www.idealibrary.com on IDEAL®

A SECTOR FOURIER p-ELEMENT APPLIED TO FREE VIBRATION ANALYSIS OF SECTORIAL PLATES

A. HOUMAT

Department of Mechanical Engineering, Faculty of Engineering, University of Tlemcen, Tlemcen 13000, Algeria. E-mail: a_houmat@mail.univ-tlemcen.dz

(*Received 22 February 2000, and in final form 9 August 2000*)

A sector Fourier p-element is presented and applied to free vibration analysis of sectorial plates. An important feature of this element is that it can describe the geometry of a sectorial plate exactly and is therefore suitable for this type of plate. The element is formulated in terms of a fixed number of cubic polynomial shape functions plus a variable number of trigonometric hierarchical shape functions. The cubic polynomial shape functions are used to describe the element's nodal d.o.f. and the trigonometric hierarchical shape functions are used to give additional freedom to the edges and the interior of the element. Results are obtained for a number of sectorial plates with various boundary conditions and comparisons are made with exact and 16-d.o.f. sector finite element solutions. The results show that the solutions converge very quickly from above to the exact values as the number of trigonometric terms is increased and highly accurate values are obtained with the use of very few terms. The results also show that the sector Fourier p-element gives a much higher accuracy than the 16-d.o.f. sector finite element with far fewer system d.o.f.

1. INTRODUCTION

This paper deals with the Fourier p-version of the finite element method applied to free vibration analysis of sectorial plates. There are a number of papers [1–4] that have suggested this method.

The Fourier p-version of the finite element method has a number of major features. The most important feature is that a simple structure such as a sectorial plate may be idealized as just one Fourier p-element and the number of trigonometric terms is varied. The results can then be obtained to any desired degree of accuracy by simply increasing the number of trigonometric terms. Another important feature is that trigonometric shape functions are used rather than forms of Legendre orthogonal polynomials which are commonly utilized in the p-version of the finite element method. The use of forms of Legendre orthogonal polynomials has the drawback that numerical rounding errors associated with floating point arithmetic increase with increasing order of polynomial [5] and thus limits the use of the method for high-frequency analysis. A sector Fourier p-element has the additional important feature of describing the geometry of a sectorial plate exactly and is therefore suitable for this type of plate.

The Fourier p-version of the finite element method has been limited currently to rectangular domains. This paper is intended to show the applicability of the method to a sectorial domain. In the sector Fourier p-element presented in this paper, the plate's transverse displacement is described by a fixed number of cubic shape functions plus a variable number of trigonometric shape functions. The cubic shape functions are used to define the element's nodal degrees of freedom (d.o.f.) and the trigonometric shape functions are used to provide additional freedom to the four edges and the interior of the element. The nodal d.o.f. and the amplitudes of the trigonometric shape functions on the four edges and in the interior of the element are used as generalized co-ordinates. The potential and kinetic energy expressions of the sector element are used in conjunction with Lagrange equations to develop the equations of motion. The resultant equations are solved as a generalized eigenvalue problem to yield the approximate frequencies.

Results of frequency calculations by use of the sector Fourier p-element are obtained for a number of sectorial plates with various boundary conditions and comparisons are made with exact and 16-d.o.f. sector finite element solutions. The 16-d.o.f. finite element used is the sector version of the 16-d.o.f. rectangular finite element of Bogner *et al.* [6].

2. FORMULATION

2.1. THE SHAPE FUNCTIONS

The shape functions will be derived for the beam Fourier p-element shown in Figure 1 (a list of nomenclature is given in Appendix A). The x co-ordinate and the non-dimensional ζ co-ordinate are related by

$$\zeta = \frac{x}{L}. \tag{1}$$

The transverse displacement w of the beam element is expressed as

$$w = c_1 + c_2\zeta + c_3\zeta^2 + c_4\zeta^3 + c_{p+4}\sin p\pi\zeta, \quad p = 1, 2, 3, \ldots. \tag{2}$$

The element's nodal d.o.f. are the transverse displacement w and the slope $w_{,x}$ at each of the two nodes. The polynomial terms on the right-hand side of equation (2) are used to describe the element's four nodal d.o.f. and the trigonometric sine terms are used to provide additional freedom to the interior of the element.

Equation (2) can be written in matrix form as

$$w = \mathbf{gc}, \tag{3}$$

where

$$\mathbf{g} = [1, \zeta, \zeta^2, \zeta^3, \sin p\pi\zeta] \tag{4}$$

and

$$\mathbf{c} = [c_1, c_2, c_3, c_4, c_{p+4}]^{\mathrm{T}}. \tag{5}$$

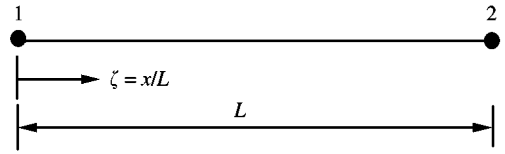

Figure 1. The beam element.

The operators $\mathbf{g}$ and $L\mathbf{g}_{,x}$ can be evaluated at each node to obtain

$$\mathbf{p} = \mathbf{hc}, \tag{6}$$

where

$$\mathbf{h} = \begin{bmatrix} 1 & 0 & 0 & 0 & 0 \\ 0 & 1 & 0 & 0 & p\pi \\ 1 & 1 & 1 & 1 & 0 \\ 0 & 1 & 2 & 3 & (-1)^p p\pi \\ 0 & 0 & 0 & 0 & 1 \end{bmatrix} \tag{7}$$

and

$$\mathbf{p} = [w_1, Lw_{1,x}, w_2, Lw_{2,x}, w_{p+4}]^{\mathrm{T}}. \tag{8}$$

The vector $\mathbf{c}$ can be obtained from equation (6) as

$$\mathbf{c} = \mathbf{h}^{-1}\mathbf{p}, \tag{9}$$

where

$$\mathbf{h}^{-1} = \begin{bmatrix} 1 & 0 & 0 & 0 & 0 \\ 0 & 1 & 0 & 0 & -p\pi \\ -3 & -2 & 3 & -1 & (2+(-1)^p)p\pi \\ 2 & 1 & -2 & 1 & -(1+(-1)^p)p\pi \\ 0 & 0 & 0 & 0 & 1 \end{bmatrix}. \tag{10}$$

Substituting equation (9) into equation (3) gives the relation

$$w = \mathbf{gh}^{-1}\mathbf{p}. \tag{11}$$

The desired shape functions $\mathbf{f}$ are therefore given by

$$\mathbf{f} = \mathbf{gh}^{-1}, \tag{12}$$

where

$$\mathbf{f} = [f_1, f_2, f_3, f_4, f_{p+4}] \tag{13}$$

and

$$f_1 = 1 - 3\zeta^2 + 2\zeta^3, \qquad f_2 = \zeta - 2\zeta^2 + \zeta^3, \qquad f_3 = 3\zeta^2 - 2\zeta^3, \qquad f_4 = -\zeta^2 + \zeta^3, \tag{14–17}$$

$$f_{p+4} = p\pi[-\zeta + (2+(-1)^p)\zeta^2 - (1+(-1)^p\zeta^3] + \sin(p\pi\zeta). \tag{18}$$

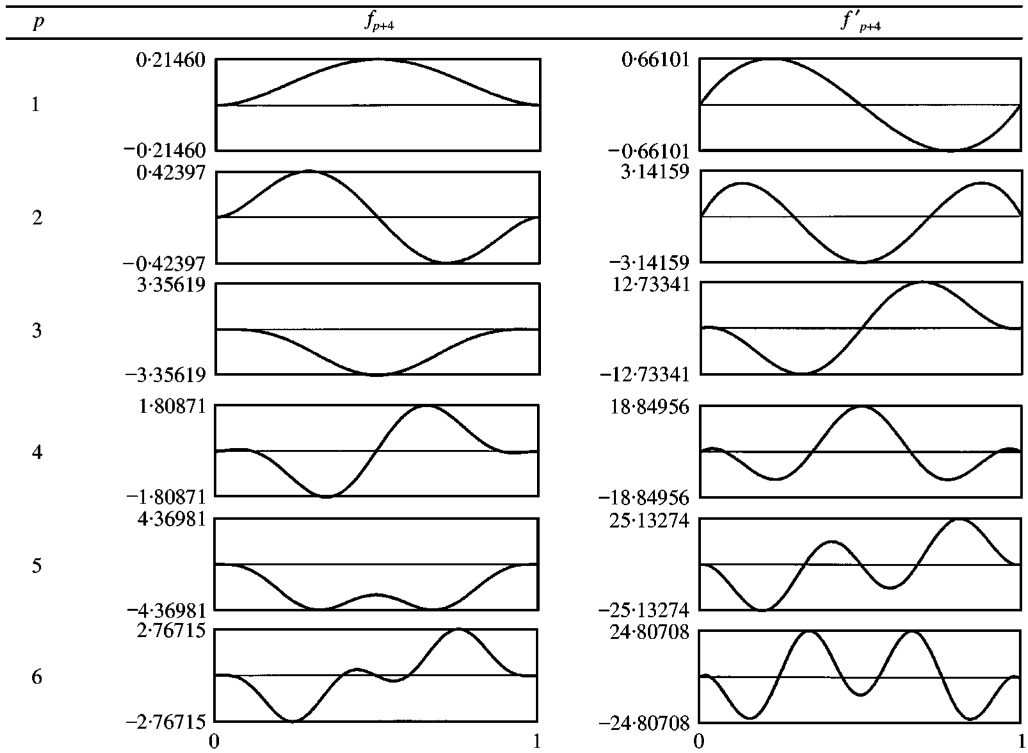

Figure 2. The first six hierarchical functions f_{p+4} and their first derivatives f'_{p+4}.

The first four shape functions are commonly used in the finite element method. The trigonometric shape functions f_{p+4} lead to zero transverse displacement and zero slope at each node. This feature is highly significant since these functions only give additional freedom to the edges and the interior of the element and do not affect the nodal d.o.f. Diagrams for the first six trigonometric shape functions $f_{p+4}(p = 1, 2, \dots, 6)$ are shown in Figure 2.

2.2. THE SECTORIAL PLATE EQUATIONS OF MOTION

An arbitrary sector plate element is shown in Figure 3. The element is bounded by concentric arcs of two circles with radii a and b $(0 < a < b)$ and two radii making an angle ϕ between them $(0 < \phi < 360^\circ)$. The polar co-ordinates r and θ and the non-dimensional ξ and η co-ordinates are related by

$$\xi = \frac{r - a}{b - a}, \quad \eta = \frac{\theta}{\phi}. \tag{19, 20}$$

The transverse displacement w can be written as

$$w(\xi, \eta, t) = \sum_{k=1}^{M+4} \sum_{l=1}^{N+4} w_{k,l}(t) f_k(\xi) f_l(\eta). \tag{21}$$

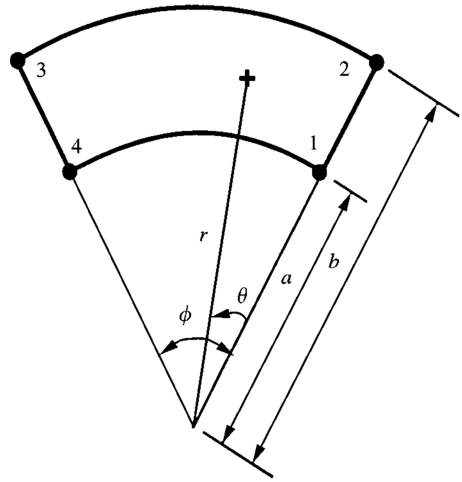

Figure 3. The sector plate element.

The strain energy U of the element is expressed as

$$U=\frac{D}{2}\int_0^1\int_0^1\left[\frac{\phi}{(b-a)^2}\left(\xi+\frac{a}{b-a}\right)\left(\frac{\partial^2 w}{\partial\xi^2}\right)^2+\frac{\phi}{(b-a)^2}\frac{1}{(\xi+a/(b-a))}\left(\frac{\partial w}{\partial\xi}\right)^2\right.$$
$$+\frac{1}{\phi^3(b-a)^2}\frac{1}{(\xi+a/(b-a))^3}\left(\frac{\partial^2 w}{\partial\eta^2}\right)^2+\frac{2\phi}{(b-a)^2}\left(\frac{\partial^2 w}{\partial\xi^2}\right)\left(\frac{\partial w}{\partial\xi}\right)$$
$$+\frac{2}{\phi(b-a)^2(\xi+a/(b-a))^2}\left(\frac{\partial w}{\partial\xi}\right)\left(\frac{\partial^2 w}{\partial\eta^2}\right)+\frac{2\nu}{\phi(b-a)^2(\xi+a/(b-a))}\left(\frac{\partial^2 w}{\partial\xi^2}\right)\left(\frac{\partial^2 w}{\partial\eta^2}\right)$$
$$-\frac{2(1-\nu)\phi}{(b-a)^2}\left(\frac{\partial w}{\partial\xi}\right)\left(\frac{\partial^2 w}{\partial\xi^2}\right)+\frac{2(1-\nu)}{\phi(b-a)^2(\xi+a/(b-a))}\left(\frac{\partial^2 w}{\partial\xi\partial\eta}\right)^2$$
$$\left.+\frac{2(1-\nu)}{\phi(b-a)^2(\xi+a/(b-a))^3}\left(\frac{\partial w}{\partial\eta}\right)^2-\frac{4(1-\nu)}{\phi(b-a)^2(\xi+a/(b-a))^2}\left(\frac{\partial^2 w}{\partial\xi\partial\eta}\right)\left(\frac{\partial w}{\partial\eta}\right)\right]\mathrm{d}\xi\,\mathrm{d}\eta. \tag{22}$$

The kinetic energy T of the element is expressed as

$$T=\frac{\rho h}{2}\phi(b-a)^2\int_0^1\int_0^1\left(\xi+\frac{a}{b-a}\right)\left(\frac{\partial w}{\partial t}\right)^2\mathrm{d}\xi\,\mathrm{d}\eta. \tag{23}$$

The motion is assumed to be harmonic and the expression for w [equation (21)] is inserted into the expressions for the strain energy U and kinetic energy T [equations (22) and (23)]. The resultant equations are then inserted into the known Lagrange equations to yield the following equations of motion for undamped free vibration;

$$\sum_{n=1}^{R}(K_{m,n}-\omega^2 M_{m,n})q_n=0,\quad m=1,2,3,\ldots,R, \tag{24}$$

in which $K_{m,n}$ are the coefficients of the stiffness matrix given by

$$K_{m,n} = D\left[\frac{\phi}{(b-a)^2} C_{i,k}^{2,2} B_{j,l}^{0,0} + \frac{\phi}{(b-a)^2} D_{i,k}^{1,1} B_{j,l}^{0,0} + \frac{1}{\phi^3 (b-a)^2} F_{i,k}^{0,0} B_{j,l}^{2,2} \right.$$
$$+ \frac{\phi}{(b-a)^2} (A_{i,k}^{2,1} + A_{i,k}^{1,2}) B_{j,l}^{0,0} + \frac{1}{\phi (b-a)^2} (E_{i,k}^{1,0} B_{j,l}^{0,2} + E_{i,k}^{0,1} B_{j,l}^{2,0})$$
$$+ \frac{\nu}{\phi (b-a)^2} (D_{i,k}^{2,0} B_{j,l}^{0,2} + D_{i,k}^{0,2} B_{j,l}^{2,0}) - \frac{(1-\nu)\phi}{(b-a)^2} (A_{i,k}^{1,2} + A_{i,k}^{2,1}) B_{j,l}^{0,0}$$
$$\left. + \frac{2(1-\nu)}{\phi (b-a)^2} D_{i,k}^{1,1} B_{j,l}^{1,1} + \frac{2(1-\nu)}{\phi (b-a)^2} F_{i,k}^{0,0} B_{j,l}^{1,1} - \frac{2(1-\nu)}{\phi (b-a)^2} (E_{i,k}^{1,0} + E_{i,k}^{0,1}) B_{j,l}^{1,1} \right] \quad (25)$$

and $M_{m,n}$ are the coefficients of the mass matrix given by

$$M_{m,n} = \rho h \phi (b-a)^2 C_{i,k}^{0,0} B_{j,l}^{0,0}. \quad (26)$$

The integrals are expressed as

$$A_{i,k}^{\alpha,\beta} = \int_0^1 f_i^\alpha f_k^\beta \,\mathrm{d}\xi, \quad (27)$$

$$B_{j,l}^{\alpha,\beta} = \int_0^1 f_j^\alpha f_l^\beta \,\mathrm{d}\eta, \quad (28)$$

$$C_{i,k}^{\alpha,\beta} = \int_0^1 (\xi + a/(b-a)) f_i^\alpha f_k^\beta \,\mathrm{d}\xi, \quad (29)$$

$$D_{i,k}^{\alpha,\beta} = \int_0^1 \frac{1}{(\xi + a/(b-a))} f_i^\alpha f_k^\beta \,\mathrm{d}\xi, \quad (30)$$

$$E_{i,k}^{\alpha,\beta} = \int_0^1 \frac{1}{(\xi + a/(b-a))^2} f_i^\alpha f_k^\beta \,\mathrm{d}\xi, \quad (31)$$

$$F_{i,k}^{\alpha,\beta} = \int_0^1 \frac{1}{(\xi + a/(b-a))^3} f_i^\alpha f_k^\beta \,\mathrm{d}\xi \quad (32)$$

in which the indices α and β ($\alpha, \beta = 0$–2) denote the order of the derivatives.

The exact values of the above integrals can easily be found by using symbolic computing which is available through a number of commercial packages.

The indices are defined as

$$i, k = 1, 2, \ldots, M+4, \qquad j, l = 1, 2, \ldots, N+4, \qquad m = j + (i-1)(N+4),$$
$$n = l + (k-1)(N+4). \quad (33\text{–}36)$$

The order R of the element stiffness and mass matrices is

$$R = (M + 4)(N + 4). \tag{37}$$

Particular boundary conditions can be specified for w, $w_{,r}$, $w_{,\theta}$, $w_{,r\theta}$ on the element's four corners, for w, $w_{,\theta}$ on the element's two edges along the r direction, and for w, $w_{,r}$ on the element's two edges along the θ direction and it is possible to accommodate any combination of corner and edge conditions in the analysis. The resultant equations can be solved as a generalized eigenvalue problem to yield the approximate frequencies ω.

3. RESULTS

Results of the application of the sector Fourier p-element to the calculation of the frequency parameters Ω were obtained for S–S–S–S, C–C–S–S, and S–C–S–S sectorial plates with $a/b = 0{\cdot}5$, $\phi = 90^\circ$, and $\nu = 0{\cdot}3$. These examples were chosen because exact solutions were available for comparison. The symbolism S–S–S–S indicates that the four edges are simply supported. The symbolism C–C–S–S indicates that the edges $r = a$, $r = b$, $\theta = 0$, and $\theta = \phi$ are clamped, clamped, simply supported, and simply supported respectively. The symbolism S–C–S–S indicates that the edges $r = a$, $r = b$, $\theta = 0$, and $\theta = \phi$ are simply supported, clamped, simply supported, and simply supported respectively.

In order to see the manner of convergence of the sector Fourier p-element solution, each sectorial plate is discretized into one element and the number of trigonometric terms is varied. An equal number of trigonometric terms is utilized in both radial and circumferential directions. Results for the 10 lowest modes of the S–S–S–S, C–C–S–S, and S–C–S–S sectorial plates are shown respectively in Tables 1–3 along with exact solutions. Blanks in these Tables are for places where there were too few system d.o.f. to be able to produce these modes. Tables 1–3 clearly show that a very fast convergence from above to the exact values occurs as the number of trigonometric terms is increased from 1 to 6 for the S–S–S–S plate, from 1 to 12 for the C–C–S–S plate, and from 1 to 10 for the S–C–S–S plate and highly accurate values are obtained with the use of very few terms. In fact, the sector Fourier p-element values agree up to three significant digits with the exact ones for all plates and for most of the modes. Tables 1–3 also show that the C–C–S–S and S–C–S–S sectorial plates which present singularities in boundary conditions required about twice as many trigonometric terms as those required by the S–S–S–S sectorial plate to obtain an equivalent accuracy.

The performance of the sector Fourier p-element with that of the 16-d.o.f. sector finite element on a system degree of freedom basis is also investigated. The 16-d.o.f. sector finite element represents the special case with no trigonometric terms ($M = N = 0$). This special finite element can also describe the geometry of a sectorial plate exactly and is therefore suitable for this type of plate. Results for the 10 lowest modes of the S–S–S–S, C–C–S–S, and S–C–S–S sectorial plates are shown respectively in Tables 4–6 along with exact solutions and solutions from the 16-d.o.f. sector finite element. The numbers of trigonometric terms M ($= N$) used in the sector Fourier p-element for the S–S–S–S, C–C–S–S, and S–C–S–S sectorial plates are 6, 12, and 10 and the corresponding numbers of system d.o.f. are 64, 168, and 132 respectively. The number of 16-d.o.f. sector finite elements used in the S–S–S–S, C–C–S–S, and S–C–S–S sectorial plates is 64 and the corresponding numbers of system d.o.f. are 256, 224, and 240 respectively. Tables 5–7 clearly show that the sector Fourier p-element produces a much higher accuracy than the 16-d.o.f. sector finite element with fewer system d.o.f. In fact, for the S–S–S–S, C–C–S–S,

Table 1

Convergence of the frequency parameters Ω for the 10 *lowest modes of the S–S–S–S sectorial plate with* $a/b = 0{\cdot}5$ *and* $\phi = 90^\circ$ (*the whole plate is discretized into one sector Fourier p-element*) *as a function of the number of trigonometric terms* M $(= N)$

$M(= N)$	1	2	3	4	5	6	7	8	9	10
1	47·096	73·213	124·529	204·593	229·697	280·854	509·385	530·688	573.951	—
2	47·089	68·384	123·638	166·482	189·601	198·440	246·793	336·166	499·166	521·529
3	47·089	68·380	103·439	166·353	189·601	198·422	228·669	294·757	332·067	364·332
4	47·089	68·380	103·437	150·983	166·352	189·599	228·653	283·599	294·750	363·965
5	47·089	68·379	103·437	150·983	166·349	189·599	209·646	228·653	283·595	354·030
6	47·089	68·379	103·437	150·982	166·349	189·599	209·646	228·652	278·386	283·593
Exact	47·089	68·379	103·437	150·982	166·348	189·599	209·646	288·652	278·386	283·593

TABLE 2

Convergence of the frequency parameters Ω for the 10 lowest modes of the C–C–S–S sectorial plate with $a/b = 0{\cdot}5$ and $\phi = 90°$ (the whole plate is discretized into one sector Fourier p-element) as a function of the number of trigonometric terms M ($= N$)

$M(=N)$	1	2	3	4	5	6	7	8	9	10
1	93·944	111·049	153·469	—	—	—	—	—	—	—
2	93·341	107·651	153·131	225·398	253·398	270·284	313·997	388·899	—	—
3	93·340	107·617	135·694	225·038	252·158	269·637	300·587	323·643	387·153	492·452
4	93·326	107·588	135·651	178·912	252·003	269·553	300·568	323·642	346·713	444·600
5	93·324	107·576	135·617	178·849	236·220	251·978	269·508	300·488	346·592	408·930
6	93·322	107·572	135·609	178·841	236·215	251·978	269·506	300·468	305.883	346·534
7	93·322	107·569	135·602	178·827	236·195	251·974	269·498	300·452	305.857	346·507
8	93·322	107·568	135·600	178·825	236·194	251·974	269·496	300·444	305.857	346·487
9	93·321	107·568	135·598	178·821	236·188	251·973	269·494	300·439	305.849	346·479
10	93·321	107·568	135·597	178·820	236·187	251·973	269·493	300·437	305.849	346·472
11	93·321	107·567	135·597	178·819	236·185	251·973	269·492	300·435	305.846	346·469
12	93·321	107·567	135·596	178·818	236·185	251·973	269·492	300·434	305.846	346·466
Exact	93·321	107·567	135·596	178·817	236·183	251·973	269·491	300·432	305.844	346·461

TABLE 3

Convergence of the frequency parameters Ω for the 10 *lowest modes of the S–C–S–S sectorial plate with* $a/b = 0{\cdot}5$ *and* $\phi = 90°$ (*the whole plate is discretized into one sector Fourier p-element*) *as a function of the number of trigonometric terms* $M\ (= N)$

$M(= N)$	1	2	3	4	5	6	7	8	9	10
1	70·345	94·310	146·105	281·701	309·860	368·208	—	—	—	—
2	70·136	89·865	144·705	211·250	222·293	231·931	284·616	371·326	627·925	654·234
3	70·136	89·858	124·316	209·243	222·274	231·055	268·334	323·064	368·516	432·700
4	70·136	89·858	124·308	172·683	209·243	231·015	268·237	321·571	323·018	426·836
5	70·136	89·858	124·308	172·683	209·232	231·010	233·306	268·237	321·566	391·091
6	70·136	89·858	124·307	172·680	209·216	231·010	233·299	268·236	304·670	321·565
7	70·136	89·857	124·307	172·680	209·215	231·009	233·298	268·236	304·665	321·564
8	70·136	89·857	124·307	172·679	209·215	231·009	233·296	268·236	304·662	321·564
9	70·136	89·857	124·307	172·679	209·214	231·009	233·296	268·236	304·661	321·563
10	70·136	89·857	124·307	172·679	209·214	231·009	233·295	268·236	304·660	321·563
Exact	70·136	89·857	124·307	172·679	209·214	231·009	233·295	268·236	304·658	321·563

Table 4

Comparison of the frequency parameters Ω for the 10 *lowest modes of the S–S–S–S sectorial plate with* $a/b = 0{\cdot}5$ *and* $\phi = 90°$. *Numbers in parentheses denote the numbers of system d.o.f.*

Type of element	1	2	3	4	5	6	7	8	9	10
Sector Fourier *p*-element (64)	47·089	68·379	103·437	150·982	166·349	189·599	209·646	228·652	278·386	283·593
Sector finite element (256)	47·089	68·383	103·491	151·307	166·387	189·635	210.865	228·718	281·823	283·894
Exact	47·089	68·379	103·437	150·982	166·348	189·599	209·646	228·652	278·386	283·593

Table 5

Comparison of the frequency parameters Ω for the 10 *lowest modes of the C–C–S–S sectorial plate with* $a/b = 0{\cdot}5$ *and* $\phi = 90°$. *Numbers in parentheses denote the numbers of system d.o.f.*

Type of element	1	2	3	4	5	6	7	8	9	10
Sector Fourier *p*-element (168)	93·321	107·567	135·596	178·818	236·185	251·973	269·492	300·434	305·846	346·466
Sector finite element (224)	93·331	107·581	135·657	179·142	237·434	252·135	269·655	300·627	309·447	346·861
Exact	93·321	107·567	135·596	178·817	236·183	251·973	269·491	300·432	305·844	346·461

Table 6

Comparison of the frequency parameters Ω for the 10 *lowest modes of the S–C–S–S sectorial plate with* $a/b = 0{\cdot}5$ *and* $\phi = 90°$. *Numbers in parentheses denote the numbers of system d.o.f.*

Type of element	1	2	3	4	5	6	7	8	9	10
Sector Fourier *p*-element (132)	70·136	89·857	124·307	172·679	209·214	231.009	233·295	268·236	304·660	321·563
Sector finite element (240)	70·138	89·862	124·363	173·021	209·293	231.082	234·594	268·335	308·328	321·887
Exact	70·136	89·857	124·307	172·679	209·214	231.009	233·295	268·236	304·658	321·563

TABLE 7

Convergence of the frequency parameters Ω for the 10 lowest modes of the S–S–S–S sectorial plate with $a/b = 0{\cdot}5$ and $\phi = 90^\circ$ (the whole plate is discretized into two sector Fourier p-elements) as a function of the number of trigonometric terms M $(= N)$ in each element

$M(=N)$	1	2	3	4	5	6	7	8	9	10
1	47·096	68·437	105·288	176·674	204·600	226·505	264·764	265·825	539·456	361·277
2	47·089	68·384	103·497	150·986	166·482	189·601	217·164	229·020	285·285	358·282
3	47·089	68·380	103·447	150·986	166·353	189·601	210·025	228·675	278·393	283·624
4	47·089	68·379	103·439	150·983	166·352	189·599	209·723	283·655	278·386	283·599
5	47·089	68·379	103·438	150·983	166·349	189·599	209·670	228·653	278·386	283·595
6	47·089	68·379	103·437	150·982	166·349	189·599	209·655	228·652	278·386	283·593
Exact	47·089	68·379	103·437	150·982	166·348	189·599	209·646	228·652	278·386	283·593

and S–C–S–S sectorial plates, the sector Fourier p-element is much more accurate than the 16-d.o.f. sector finite element although it has respectively about 75, 25, and 45% fewer system d.o.f.

Situations may arise in which a sectorial plate is made of two or more different materials and/or edges which have two or more different boundary conditions. If this is the case then the plate must be discretized into two or more elements. The applicability of the sector Fourier p-element to such a case will be shown by considering an S–S–S–S sectorial plate with $a/b = 0{\cdot}5$, $\phi = 90^\circ$, and $\nu = 0{\cdot}3$. In order to see the manner of convergence of the sector Fourier p-element solution, the sectorial plate is discretized into two identical elements each with $\phi = 45^\circ$ and an equal number of trigonometric terms $M(= N)$ is used in both elements. Inter-element compatibility is achieved by matching the displacements, rotations, and warps at the nodes and the amplitudes of the trigonometric shape functions at the edges. Results for the 10 lowest modes are shown in Table 7 along with the exact values. Table 7 clearly shows that a very fast convergence from above to the exact values occurs as the number of trigonometric terms is increased from 1 to 6 and the values for $M = N = 6$ are in excellent agreement with the exact ones.

4. CONCLUSION

A sector Fourier p-element has been presented and applied to free vibration analysis of sectorial plates. The element is formulated in terms of a fixed number of cubic polynomial shape functions plus a variable number of trigonometric shape functions. A major feature of this element is that it can describe the geometry of a sectorial plate exactly and is therefore suitable for this type of plate. Results of frequency calculations were found for a number of sectorial plates with various boundary conditions and comparisons were made with exact and 16-d.o.f. sector finite element solutions. The results of the sector Fourier p-element were found to converge very quickly to the exact values as the number of trigonometric terms increased and highly accurate values were obtained with the use of very few terms. When compared with the 16-d.o.f. sector finite element, the sector Fourier p-element was found to yield a much higher accuracy with far fewer system d.o.f. The applicability of the sector Fourier p-element to cases where two or more elements are necessary has been demonstrated by considering a simply supported sectorial plate discretized into two identical sector Fourier p-elements and highly accurate values were found with the use of very few trigonometric terms.

REFERENCES

1. A. HOUMAT 1997 *Journal of Sound and Vibration* **206**, 201–215. An alternative hierarchical finite element formulation applied to plate vibrations.
2. O. BESLIN and J. NICOLAS 1997 *Journal of Sound and Vibration* **202**, 633–655. A hierarchical functions set for predicting very high order plate bending modes.
3. N. S. BARDELL, J. M. DUNSDON and R. S. LANGLEY 1997 *Composite Structures* **38**, 463–475. Free vibration of coplanar sandwich panels.
4. A. Y. T. LEUNG and J. K. W. CHAN 1998 *Journal of Sound and Vibration* **212**, 179–185. Fourier p-element for the analysis of beams and plates.
5. L. J. WEST, N. S. BARDELL, J. M. DUNSDON and P. M. LOASBY 1997 *The Sixth International Conference on Recent Advances in Structural Dynamics, Southampton*, 217–227. Some limitations associated with the use of K-orthogonal polynomials in hierarchical versions of the finite element method.
6. F. K. BOGNER, R. L. FOX and L. A. SCHMIT 1965 *The First Conference on Matrix Methods in Structural Mechanics, Ohio*, 397–443. The generation of inter-element compatible stiffness and mass matrices by the use of interpolation formulas.

APPENDIX A: NOMENCLATURE

a	inner radius
b	outer radius
h	thickness
ϕ	angle between the two bounding radii
ρ	mass density
E	modulus of elasticity
v	Poisson's ratio
D	flexural rigidity $[Eh^3/(12(1-v^2))]$
r, θ	polar co-ordinates
ξ, η	non-dimensional co-ordinates
t	time
w	transverse displacement
$w_{,r}$	rotation about θ-axis
$w_{,\theta}$	rotation about r-axis
$w_{,r\theta}$	warp
U	strain energy
T	kinetic energy
$K_{m,n}$	coefficients of stiffness matrix
$M_{m,n}$	coefficients of mass matrix
q_n	coefficients of vector of generalized co-ordinates
M	number of trigonometric terms in radial direction
N	number of trigonometric terms in circumferential direction
R	order of stiffness and mass matrices
ω	natural frequency
Ω	frequency parameter $(\omega b^2\sqrt{\rho h/D})$